Ultrasonics 53 (2013) 1089–1096

Contents lists available at SciVerse ScienceDirect

Ultrasonics

journal homepage: www.elsevier.com/locate/ultras

Ultrasonic assisted-ECAP

F. Djavanroodi [a,*], H. Ahmadian [b], K. Koohkan [b], R. Naseri [b]

[a] Department of Mechanical Engineering, Qassim University, Qassim, Saudi Arabia
[b] Department of Mechanical Engineering, Iran University of Science and Technology, Tehran, Iran

ARTICLE INFO

Article history:
Received 3 May 2012
Received in revised form 3 February 2013
Accepted 4 February 2013
Available online 22 February 2013

Keywords:
ECAP
Ultrasonic vibration
FEM
Amplitude
Frequency

ABSTRACT

Equal channel angular pressing (ECAP) is one of the most prominent procedures for achieving ultra-fine grain (UFG) structures among the various severe plastic deformation (SPD) techniques. In this study, the effect of ultrasonic vibration on deformation behavior of commercial pure aluminum in the ECAP process is analyzed successfully using three dimensional (3D) by finite element methods (FEMs). The investigation includes the effects of die geometry, billet length, friction factor, ram speed, ultrasonic amplitude and ultrasonic frequency. Conventional as well as ultrasonic ECAP has been performed on aluminium 1070 alloy and the obtained data were used for validating simulations. It is observed that a 13% reduction in the average force was achieved when ultrasonic vibration with amplitude of 2.5 μm at 20 kHz is applied. Also, further reduction in ECAP forming forces are obtained with increase of vibration amplitude, vibration frequency, friction factor, billet length and die channel angle.

1. Introduction

Severe plastic deformation by ECAP is one of the most attractive ways to fabricate ultra-fine grain structures and increase the strength of metals and alloys [1,2]. In the this process, a cylindrical or square shape sample is pressed through a die with two identical cross-sections channels intersecting at a die channel angle of φ and a corner angle of ψ. During deformation the billet undergoes an intense plastic strain through simple shear [3]. The magnitude of effective strain (ε_{eq}) after N passes in frictionless conditions imposed on ECAPed material is given by the following relationship [3]:

$$\varepsilon_{eq} = N/\sqrt{3}\left[2\cot\left(\frac{\varphi+\psi}{2}\right)+\psi\cos ec\left(\frac{\varphi+\psi}{2}\right)\right] \quad (1)$$

Eq. (1) represents the average equivalent strain developed in the sample within frictionless condition but friction between the surface of the sample and the die wall is unavoidable in the practical ECAP process. ECAP is considered to be friction sensitive process and there have been several studies regarding the effect of friction on the deformation behavior during the process [1,4–10]. Prangnell et al. [4], has shown that strain and inhomogeneous deformation increases with friction. Nagasekhar et al. [8], has reported that increasing the corner angle reduces the friction force in the ECAP process because it reduces the contact surface between the material and the die in the shear deformation zone. Eivani et al. [9], and Eivani and Karimi Taheri [10], have shown that increasing the friction factor increases the forming force strongly and also, there exists a critical friction factor in which, dead metal zone are formed during the forming process. Luis-Pérez's et al. [11], has shown that die channel angle and friction condition are critical factors in the effective strain and forming force. Forming force in the ECAP Process (F) using upper-bound analysis is represented in Eq. (2) [12]:

$$F = a^2\tau_0(1+m)\left[2\cot\left(\frac{\varphi+\psi}{2}\right)+\psi\right]+4ma\tau_0(l_i+l_0) \quad (2)$$

where φ, ψ, a, l_i, l_o, m, τ_o are the channel angle, the corner angle, the width of the ECAP channel, instant length of the sample in the entry channel, instant length of the sample in the exit channel, the friction and the shear strength, respectively. Eq. (2) shows that the forming load in the ECAP process decreases with reducing friction factor, thus it is crucial to decrease the sliding friction between the workpiece and the die especially in the entrance channel.

The effect of ultrasonic energy on the deformation behavior of metals and alloys has been under investigation in recent years. Blaha and Langenecker were the first to investigate the effects of ultrasonic vibration on the plastic deformation of metals [13,14]. Also, methods have been developed to utilize ultrasonic vibration during manufacturing process such as wire drawing, extrusion, upsetting and deep drawing [15–25]. The application of high frequency ultrasonic energy to the specimen during tension and compression tests reduces the yield strength of the material. This is due to acoustic softening (similar to thermal softening) which happens during application of ultrasonic vibration to the metal forming process. Experimental results revealed that the ultrasonic energy required to produce the same amount of softening is 10^7 times less than the required thermal energy. The reason is that ultrasonic

* Corresponding author. Tel.: +966380005308
E-mail address: roodi@qec.edu.sa (F. Djavanroodi).

0041-624X/$ - see front matter © 2013 Elsevier B.V. All rights reserved.
http://dx.doi.org/10.1016/j.ultras.2013.02.003

energy is only absorbed in localized regions, such as vacancies, dislocations and grain boundaries, while thermal energy is absorbed uniformly in the material. Acoustic softening effect is proportional to the applied ultrasonic intensity [15]. Ashida and Aoyama [16] performed experimental and numerical studies of ultrasonic assisted press forming. They showed that ultrasonic energy helps to reduce wrinkling and cracking. The results showed that this was achieved by reducing the friction force between the sheet metal and the die. Huang et al. [22,23] showed that, ultrasonic vibration can reduce the average forming force during the hot and cold upsetting processes due to the decrease in friction force. Inoue [24] performed experimental studies on ultrasonic assisted metal tube drawing and found that, for thick steel tubes, no significant reduction in drawing force was observed. Most studies on the effect of ultrasonic vibrations on the metal forming processes reach the same conclusions, that is: ultrasonic vibrations causes' reduction in forming force, flow stress, friction between tool and workpiece, surface quality and internal structure defects generation [17,18]. One of the factors in loss of forming energy is friction, so it is very significant that sliding friction between the workpiece and the tool is reduced in the metal forming processes. The influence on sliding friction of ultrasonic vibration both parallel and perpendicular to the sliding direction has been studied for samples of aluminium alloy sliding against tool steel by Kumar et al. [26]. Experiments were performed at a mean sliding speed and at mean contact pressure with ultrasonic vibration and significant reduction in sliding friction were observed. Furthermore, it is shown that the reduction in friction by longitudinal vibration was greater than by transverse vibration.

In the present paper, AA 1070 aluminium was ECAPed one pass and the obtained data were used for validating the FEM model. Then finite element simulations were conducted to explore the frictional effect of superimposing ultrasonic-vibration during ECAP process. The objective of this study is to explore the effects of ultrasonic vibration on the reduction of ECAP forming load. The parameters which have been considered are: ultrasonic amplitude; ultrasonic frequency; rams speed; friction factor; billet length and die channel angle. No attempted has been made to account for acoustic softening effects. Kumars [26] friction model is used for this investigation.

2. Finite element methods

In this study a three dimensional finite element modelling with ABAQUS/CAE was used to investigate the ECAP process. In the first step a conventional and ultrasonic ECAP for aluminium 1070 alloy was modelled and validated with experimental data. The Hydraulic press set-up and ECAP circular cross section die with $\varphi = 90^\circ$ and $\psi \approx 15^\circ$ which are used for the experimental work are shown in Fig. 1. Experimental condition, specimen dimensions, material composition and material properties are shown in Tables 1–3. In the second step a longitudinal ultrasonic vibration was applied to the specimen for investigating its effect on forming force.

Table 1
Experimental conditions.

Experiment condition		Billet dimension		Die dimension	
Friction	Ram speed (mm/s)	Billet diameter (mm)	Billet length (mm)	90°	φ
0.12	2	20	150	15°	ψ
				20	Die diameter (mm)

2.1. Modelling

A 3D FEM model of specimen with same dimensions as the workpice was constructed. The die and ram were assumed rigid and billet was assumed deformable. Die and ram modelled by four-node bilinear rigid quadrilateral (R3D4) elements and eight-node linear brick, reduced integration and hourglass control (C3D8R) are applied to model the aluminium specimen. The plastic deformation behaviour of the material follow the relationship $\sigma = C\varepsilon^n$ where σ is the effective von-misses stress, ε is the effective plastic strain, C is the strength coefficient and n is strain hardening exponent respectively. Tensile test were performed to determine the strength coefficient and strain hardening exponent according to ASTM B557 M (2006) for Al 1070 and the equation $\sigma(\text{Mpa}) = 104.3\ \varepsilon^{0.168}$ was obtained. The contact between the surface of the rigid die and the specimen is modelled as surface-to-surface contacts and a finite amount of sliding between the surfaces were allowed. The frictional behaviour of the contact pairs is assumed to follow Coulomb's model. The magnitude of friction in the simulation was assumed 0.12 [25]. The punch speed was 2 mm/s and all of the simulations were performed at room temperature. The workpiece volume was meshed by 0.0026 mesh size which is achieved with mesh sensitivity diagram. The automatic re-meshing was applied in case the elements became too distorted during the ECAP simulation.

2.2. Validation of simulation analysis

To validate simulation results, ECAP die with the die channel angle of 90° and outer corner of 15° was used. Aluminium 1070 alloy was used that was homogenized at 670 °C for 0.5 h. The maximum punch force is a very significant parameter in the experiment to be considered for selecting the suitable hydraulic press in designing the ECAP setup. For the experimental ultrasonic

Fig. 1. Hydraulic press set-up and ECAP die with $\varphi = 90^\circ$ and $\psi \approx 15^\circ$.

Table 2
Chemical composition of commercial pure aluminium.

Material component	Aluminium, Al	Iron, Fe	Vanadium, V	Gallium, Ga	Zinc, Zn	Titanium, Ti	Magnesium, Mg	Stannum, Sn
Percent	99.737	0.127	0.012	0.011	0.009	0.002	0.03	0.043

Table 3
Hardening properties.

$\sigma = K\varepsilon^n$	
n, Strain hardening exponent	K (MPa), strength coefficient
0.168	104.3

condition the press punch (ram) was vibrated with vibration amplitude of 2.5 μm at 20 kHz. Also, similar condition was assumed for simulation (see Fig. 2). MoS2 was used as lubrication. The magnitude of the friction coefficient in the simulation condition was assumed as 0.12 [1]. The ECAP force increases gradually with the ram movement until shear strain imposed to the sample. From this point (maximum punch pressure), the pressing pressure decreases with a very slow rate which continuous to the end of the process; because of decreasing the billet length and friction force. From experimental work it was found that the maximum required forming forces to conduct the conventional and ultrasonic ECAP processes are 162.5 KN and 147.9 KN respectively. The maximum forming force magnitudes obtained from simulation result for conventional and ultrasonic ECAP processes are 155.5 KN and 137 KN respectively. The results present a 4.3% (conventional ECAP) and 7.3% (ultrasonic ECAP) discrepancy between the experimental and the numerical result, which for all practical purposes is acceptable.

3. Friction model

There are two main types of friction that are commonly encountered: dry friction and fluid friction. Dry friction, also called 'Coulomb' friction, explains the tangential component of friction force between two surfaces that move relative to each other. Fluid friction is related to the contact friction force between adjacent layers of fluid move that with different velocities relative to each other. If it is assumed that the friction force is independent of contact area The relation between the magnitude of velocity and friction can be described by the following equation [27]:

$$F = F_T \mathrm{sgn}(V) \tag{3}$$

where F_T is proportional to the normal load i.e. $F_T = \mu F_N$ and V is total velocity. The Coulomb model however does not specify the friction force at zero velocity.

Vibrating and sliding velocities are shown in Fig. 3. The total velocity is given by [27]:

$$V_{\text{total}} = V_S + V_{\text{vib}} \cos(\omega t) \tag{4}$$

$V_s$is the sliding velocity, V_{vib} is the velocity of vibration and ω is the angular frequency of vibration. Fig. 4 shows the instantaneous friction force with time over one cycle of vibration given by the following equation [27]:

$$F = F_T \mathrm{sgn}(V_S + V_{\text{vib}} \cos(\omega t)) \tag{5}$$

Kumar [26] has proposed Eq. (6) for reduction of friction force by longitudinal vibration. During the interval OE, friction force over the times AB and CD is exactly equal but direction of it will oscillate between angles $(-\pi)$ and $(+\pi)$ to sliding velocity. Thus an average frictional force over one cycle of vibration (F) is given by the following equation [26]:

$$F = F_T\left(\frac{2}{\pi}\sin^{-1}\left(\frac{V_s}{a\omega}\right)\right) \tag{6}$$

Reduction of friction force in this theory is independent of parameters such as mass, stiffness, coefficient of friction, tangential contact stiffness. It solely depends on the ratio of the sliding velocity to the vibration velocity [26].

4. Superimposing ultrasonic vibration

The influence of ultrasonic vibration (parallel and perpendicular to the sliding direction) on sliding friction has been studied in the ECAP process. The aluminium alloy samples slides against tool steel. The vibration can be superimposed to die or billet. According

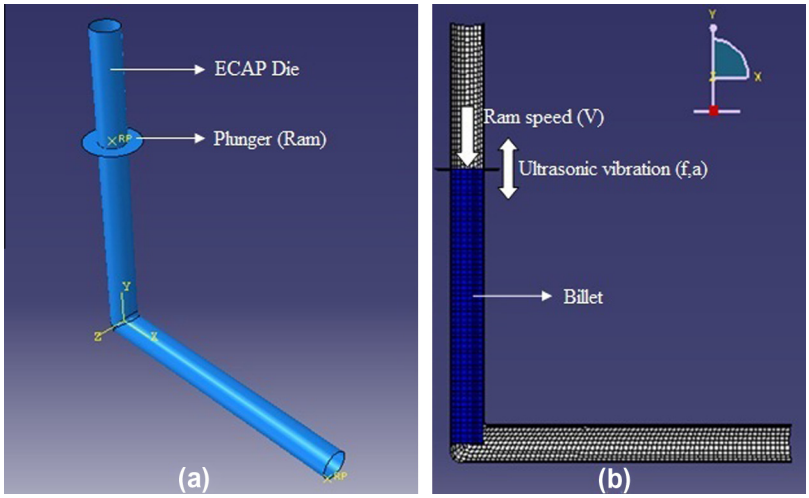

Fig. 2. Modelling (a) FEM model, (b) Applying the ultrasonic vibration and velocity on the plunger.

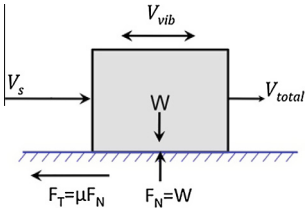

Fig. 3. Coulomb friction model [27].

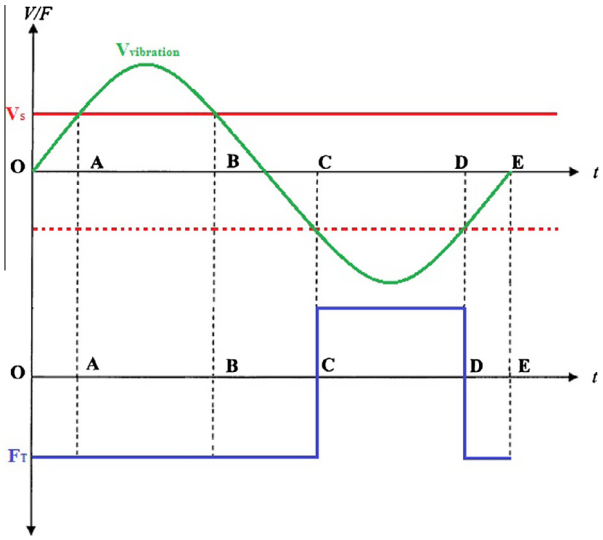

Fig. 4. Variation of vibration velocity with time over one cycle of vibration and corresponding change in direction of frictional force [26].

to geometry, size and constraints of ECAP dies it's unpractical to apply vibration to die. Also, it has been shown that the reduction in friction by longitudinal vibration is much greater than by transverse vibration [26]. Therefore, longitudinal ultrasonic vibrations were superimposed to the billet. To decrease the run time of simulations the ram speed was increased from 2 mm/s to 100 mm/s while all the other parameters were kept constant [16]. Hence, the simulated ECAP process was performed with a constant ram speed of 100 mm/s while press punch (ram) was vibrated with vibration amplitude 2.5 μm at 20 kHz-periodic term. In the simulations, for every excitation frequency it is assumed that the excitation frequency is close to the natural frequency of set-up. Plunger (ram) is modelled as a shell and ultrasonic vibration is applied on it. Ultrasonic vibration was imposed to the billet longitudinally (axial direction). Fig. 5 shows the dimension of H13 steel horn designed and manufactured for applying the ultrasonic vibration. The ultrasonic generator with 20 kHz frequency and maximum capacity of 2 KW was used to provide the required power for ultrasonic oscillation. The horn was considered resonant in a longitudinal mode and connected to the transducer and billet. The dimensions of the horn were designed so that natural frequency of tooling system is close to the imposed frequency. Finite element analysis and modal analysis were employed to determine the dimensions of the horn. The length of the horn is equal to the wavelength of the transmitted wave. The horn was held at a position with zero amplitude node, and maximum amplitude were at the interface of horn/transducer and horn/billet. In order to study the effect of the amplitude and frequency on the applied load, different amplitudes of 2.5, 5, 10, 15, 20, and 25 μm at constant frequency 20 kHz and different frequencies of 10, 15, 20, 25 and 30 kHz at constant amplitude 2.5 μm were simulated respectively. Furthermore, the effects of ECAP parameters such as, friction factor, billet length and die channel angle on ultrasonic-ECAP force were also studied. It should be noted that the die geometry (channel angle (φ), corner angle (ψ)) were kept constant during the simulations.

5. Results and discussion

5.1. The effect of ultrasonic vibrations on the ECAP force

The effect of ultrasonic vibrations on the ECAP force is investigated by imposing the axial ultrasonic vibrations on the billet while ram speed was 2 mm/s. To validate the simulation results, a comparison has been made between the maximum load obtained by conventional and ultrasonic ECAP process and the finite element simulation. Fig. 6 shows that a good agreement was obtained between the numerical and experimental result. Similar simulation conditions were applied to the conventional and axial ultrasonic vibrations ECAP process. For the ultrasonic-ECAP process vibration were applied to the ram by a harmonic function. The reduction of the external load due to applying the ultrasonic vibration is shown in Fig. 6. Table 4 shows the magnitude of the experimental and numerical forming force for conventional and ultrasonic ECAP. The results show that a 9% and 13% reduction in the forming force was obtained with experimental and simulated ultrasonic-ECAP respectively.

5.2. The effect of the ram speed on the ECAP force

For sinusoidal vibration of the ram, there exists a critical speed in which there is no reduction in forming force when the ram speed is more than the critical speed in the analysis. The maximum vibration speed (critical speed) is equal to $V_{cr} = 2\pi af$, where a and f are amplitude and the frequency respectively. For this study $a = 2.5$ μm and $f = 20$ kHz, therefore the critical ram speed is $V_{cr} = 314$ mm/s. The effect of ram speed on ECAP forming force is shown in Fig. 7. As it can be seen, ECAP forming force is decreased with increasing the velocity ratio (ratio of the sliding velocity to the vibration velocity). This was achieved by reducing the time interval (i.e. AB = CD) see Fig. 6, by increasing the ram speed.

5.3. The effect of ultrasonic vibrations amplitude

In this part the effect of vibration amplitude variations were investigated while all the other parameters were remained constant. The vibration frequency was kept at 20 kHz and the amplitudes were 2.5, 5, 10, 15, 20, 25 μm. Simulation results shows that the ECAP load decreases with increasing the vibration amplitude (see Fig. 8). Fig. 9 shows the percentage reduction in forming loads with respect to amplitudes, as it can be seen increasing the ultrasonic vibration amplitudes, increases the friction force inversion time per vibration cycle, therefore, ECAP load decreases.

5.4. The effect of ultrasonic vibrations frequency

The effect of ultrasonic vibration frequencies (10, 15, 20, 25, 30 kHz) on forming force is investigated while the amplitude of vibration was constant at 2.5 μm. Simulation results show that, the forming load decreases with the increase of vibration frequencies (Fig. 10). Fig. 11 shows the percentage reduction in forming loads for different frequencies, as it can be seen the vibration amplitude has more influence on force reduction than the vibration frequency in ECAP process.

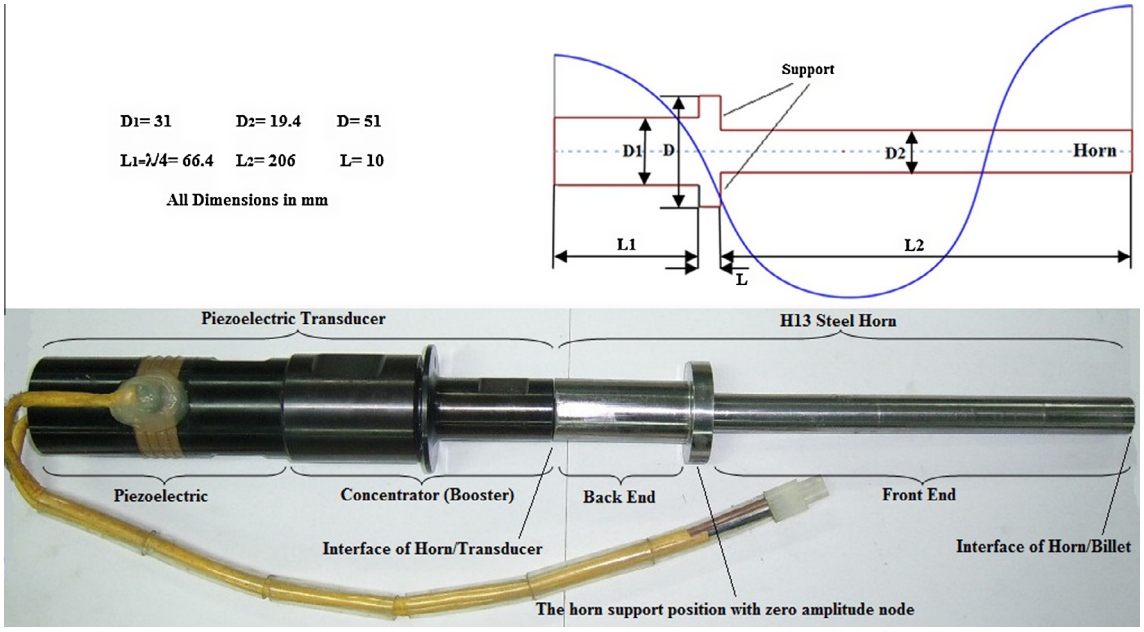

Fig. 5. Dimensions of H13 steel Horn.

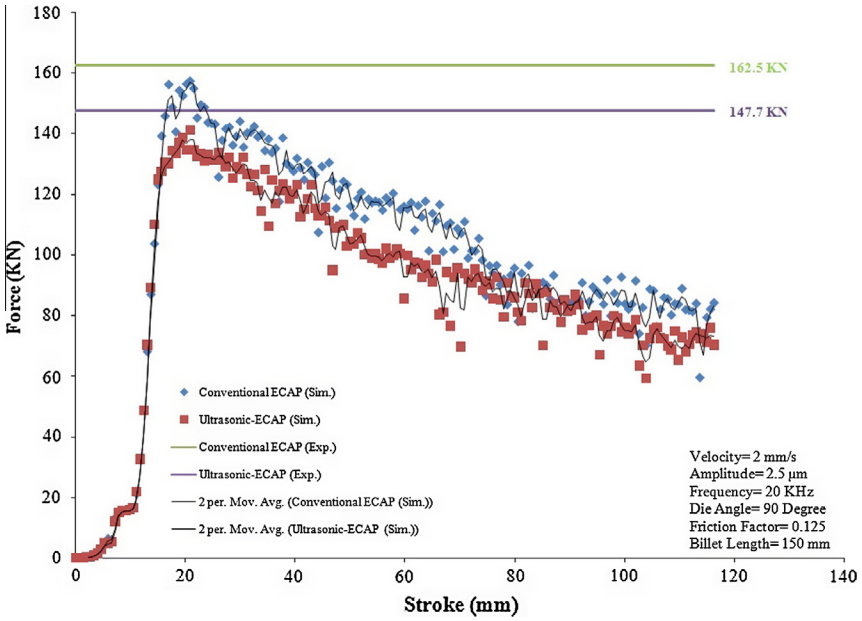

Fig. 6. Comparison of experimental and numerical ECAP forming force.

Table 4
Magnitude of the experimental and numerical forming force for conventional and ultrasonic ECAP.

Process	Maximum force (KN)		Error (%)
	Experiment	Simulations	
Conventional ECAP	162.5	157.5	3.1
Ultrasonic-ECAP	147.7	137	7.3
Force reduction (%)	9.1	13	

5.5. The effect of friction factor

The effect of different friction factors on ECAP forming force and percentage forming force reduction are shown in Figs. 12 and 13 respectively. In the analysis the friction factor is changed from 0.05 to 0.2 and the amplitude and frequency of vibration were kept constant at 2.5 μm and 20 kHz respectively. Results indicate that, with increasing the friction factor the share of friction force in the total forming force increases. Hence, the percentage ECAP forming force reduction increases.

5.6. The effect of billet length on Ultrasonic-ECAP

Billet length varies during the ECAP process. Figs. 14 and 15 presents the effect of billet length on forming loads and percentage forming force reduction in ultrasonic-ECAP. Results show that more reduction in forming load is achieved with increasing billet length. With higher billet length the total forming load increases.

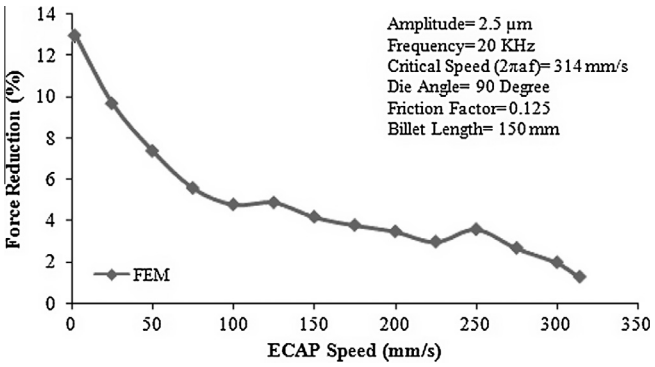

Fig. 7. The effect of ram speed on ECAP forming force.

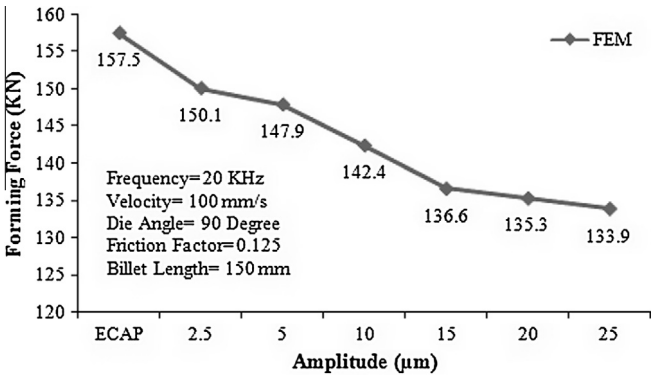

Fig. 8. The effect of vibration amplitude on punch force.

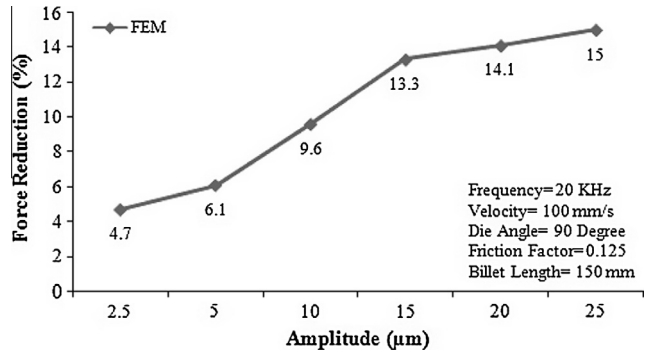

Fig. 9. Percentage reduction in forming loads with respect to amplitudes.

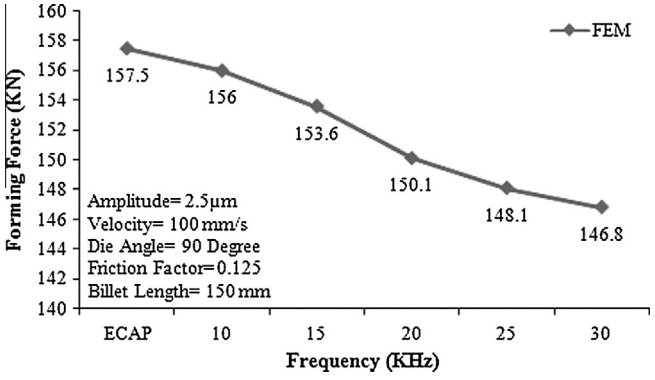

Fig. 10. The effect of vibration frequency on forming force.

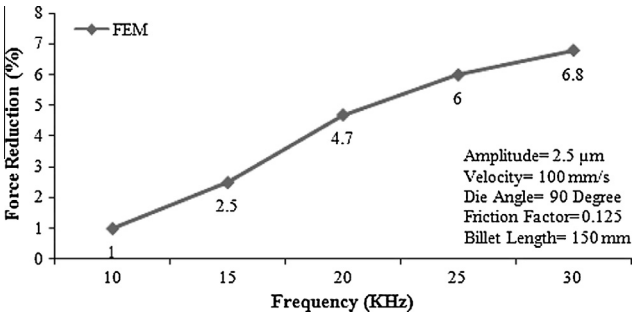

Fig. 11. Percentage reduction in forming loads for different frequencies.

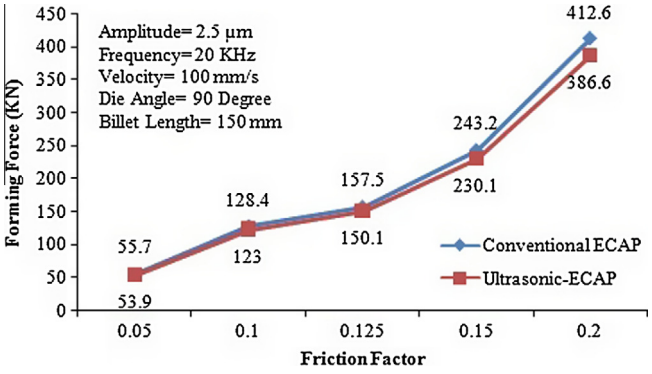

Fig. 12. ECAP forming force reduction at different friction factors.

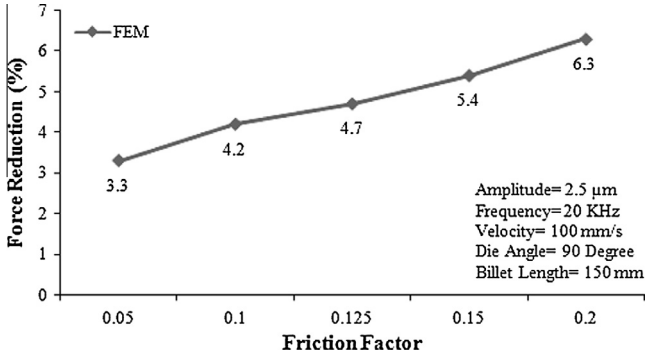

Fig. 13. ECAP forming force reduction percentage at different friction factors.

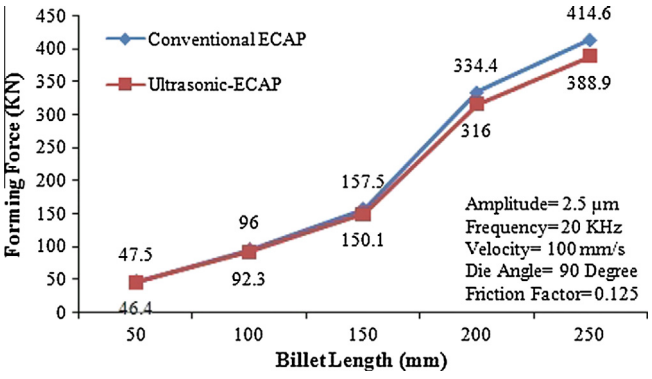

Fig. 14. The effect of billet length on forming load.

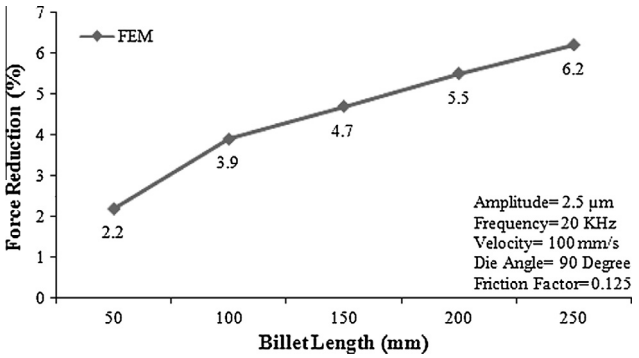

Fig. 15. The effect of billet length on percentage reduction of forming force.

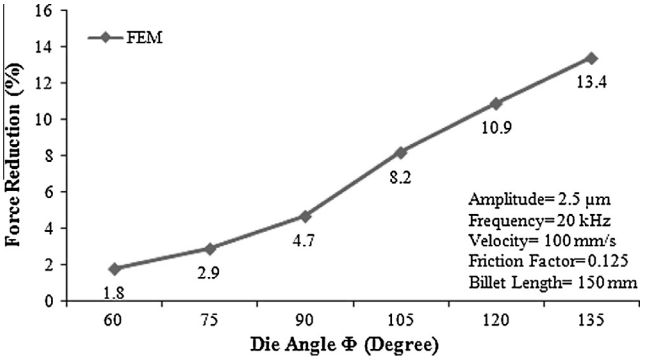

Fig. 16. The influence of die channel angle on ultrasonic ECAP.

Since the shear force remains constant in the process, so that the increase in total forming load is mainly due to frictional force. Hence, as the billet length increases the percentage ECAP forming force reduction increases.

5.7. The effect of die channel angle (φ) on Ultrasonic-ECAP

Fig. 16 shows the influence of die channel angle on ultrasonic-ECAP. Die channel angle (φ) of 60°, 75°, 90°, 105°, 120° and 135° were analysed. As shown in Fig. 16 forming force decreases with increasing die channel angle. The shearing force decreases as the die channel angle increases and the frictional force becomes a larger portion of total forming load. Also as channel angle becomes larger the ultrasonic vibration will have more influence on the frictional force in the outer die channel. Hence, larger reduction in forming is achieved with higher die channel angle.

5.8. Future work

In addition to the numerical analysis used in this paper regarding effects of ultrasonic vibration on ECAP process, a new experimental setup has been designed and manufactured to make use of ultrasonic vibration in ECAP process. This setup was used to verify the numerical findings of this paper.

6. Conclusion

Finite element analyses were performed to simulate a conventional and ultrasonic-ECAP. Conventional and ultrasonic ECAP processes were validated with experimental data. The critical findings of this study can be summarized as follows:

1. ECAP forming force is reduced by 9% when ultrasonic vibration were introduced.
2. For velocity ratio (ratio of the sliding velocity to the vibration velocity) less than 1, simulation results show that superimposing ultrasonic vibration cause a reduction in ECAP force; due to reduction in friction force and flow stress.
3. ECAP forming force is reduced when amplitude or frequency of vibration were increased. The vibration amplitude has more effective than frequency in reducing the forming load.
4. Reduction of forming force of 6% was obtained with increasing the friction factor from 0.05 to 0.2.
5. It was found that 4% increase in reduction in forming force was achieved with increasing the billet length from 50 mm to 250 mm.
6. A maximum of 13% reduction in forming force is achieved with increasing the die channel angle from 60° to 135°.

Acknowledgements

The authors would like to thank the *Tirage Machine* for their supports.

References

[1] F. Djavanroodi, M. Ebrahimi, Effect of die channel angle, friction and back pressure in the equal channel angular pressing using 3D finite element simulation, Materials Science and Engineering A 527 (2010) 1230–1235.
[2] A.V. Nagasekhar, T. Rajkumar, D. Stephan, Y. Tick-Hon, R.K. Guduru, Microstructure and mechanical properties of pure gold processed by equal channel angular pressing, Materials Science and Engineering A 524 (2009) 204–207.
[3] Y. Iwahashi, J. Wang, Z. Horita, M. Nemoto, T.G. Langdon, Scripta Materialia 35 (1996) 143.
[4] P.B. Prangnell, C. Harris, S.M. Roberts, Finite element modeling of equal channel angular extrusion, Scripta Materialia 37 (7) (1997) 983–989.
[5] I. Balasundar, T. Raghu, Effect of friction model in numerical analysis of equal channel angular pressing process, Materials and Design 31 (2010) 449–457.
[6] I. Balasundar, M. Sudhakara Rao, T. Raghu, ECAP die to extrude a variety of materials, Materials and Design 30 (2009) 1050–1059.
[7] S. Dumoulin, H.J. Roven, J.C. Werenskoid, H.S. Valberg, Finite element modeling of equal channel angular pressing: effect of material properties, friction and die geometry, Materials Science and Engineering A 410–411 (2005) 248–251.
[8] A.V. Nagasekhar, S.C. Yoon, Y. Tick-Hon, H.S. Kim, An experimental verification of the finite element modeling of equal channel angular pressing, Computational Materials Science 46 (2009) 347–351.
[9] A.R. Eivani, S. Ahmadi, E. Emadoddin, S. Valipour, A. Karimi Taheri, The effect of deformations passes on the extrusion pressure in axi-symmetric equal channel angular extrusion, Computational Materials Science 44 (2009) 1116–1125.
[10] A.R. Eivani, A. Karimi Taheri, The effect of dead metal zone formation on strain and extrusion force during equal channel angular extrusion, Computational Materials Science 42 (2008) 14–20.
[11] C.J. Luis-Pérez, R. Luri-Irigoyen, D. Gaston-Ochoa, Journal of Materials Processing Technology 153–154 (2004) 846–852, http://dx.doi.org/10.1016/j.jmatprotec.2004.04.115).
[12] A.R. Eivani, A. Karimi Taheri, An upper bound solution of ECAE process with outer curved corner, Journal of Materials Processing Technology 182 (2007) 555–563.
[13] F. Blaha, B. Langenecker, Naturwissenschaften 42 (1955) 556.
[14] B. Langenecker, Effects of ultrasound on deformation characteristics of metals, IEEE Transactions on Sonics and Ultrasonics 13 (1966) 1–8.
[15] A. Siddiq, T. El Sayed, Ultrasonic-assisted manufacturing processes: variational model and numerical simulations, Ultrasonics 52 (2012) 521–529.
[16] Y. Ashida, H. Aoyama, Press forming using ultrasonic vibration, Journal of Materials Processing Technology 187–188 (2007) 118–122.
[17] J.C. Hung, Y.C. Tsai, C. Hung, Frictional effect of ultrasonic-vibration on upsetting, Ultrasonics 46 (2007) 277–284.
[18] C. Bunget, G. Ngaile, Influence of ultrasonic vibration on micro-extrusion, Ultrasonics 51 (2011) 606–616.
[19] B.N. Mordyuk, V.S. Mordyuk, V.V. Buryak, Ultrasonic drawing of tungsten wire for incandescent lamps production, Ultrasonics 42 (2004) 109–111.
[20] M. Murakawa, M. Jin, The utility of radially and ultrasonically vibrated dies in the wire drawing process, Journal of Materials Processing Technology 113 (2001) 81–86.
[21] S.A.A. Akbari Mousavi, H. Feizi, R. Madoliat, Investigations on the effects of ultrasonic vibrations in the extrusion process, Journal of Materials Processing Technology 187–188 (2007) 657–661.

[22] Z. Huang, M. Lucas, M.J. Adams, Influence of ultrasonics on upsetting of a model paste, Ultrasonics 40 (2002) 43–48.
[23] J.C. Hung, C. Hung, The influence of ultrasonic-vibration on hot upsetting of aluminum alloy, Ultrasonics 43 (2005) 692–698.
[24] M. Inoue, Studies on ultrasonic metal tube drawing, Memoira of Sagami Institute of Technology 19 (1984) 1–7.
[25] T. Jimma, Y. Kasuga, N. Iwaki, O. Miyazawa, E. Mori, K. Ito, H. Hatano, An application of ultrasonic vibration to the deep drawing process, Journal of Materials Processing Technology 80–81 (1998) 406–412.
[26] V.C. Kumar, I.M. Hutchings, Reduction of the sliding friction of metals by the application of longitudinal or transverse ultrasonic vibration, Tribology International 37 (2004) 833–840.
[27] Sh. Bharadwaj, Active Friction Control via Piezoelectrically Generated Ultrasonic Vibrations, Master of Science, The Graduate School of the Ohio State University, 2009.